



**HAL**  
open science

# A Multi-Objective Metamodel-Assisted Memetic Algorithm with Strength-based Local Refinement

Kyriakos C. Giannakoglou, Chariklia Georgopoulou

► **To cite this version:**

Kyriakos C. Giannakoglou, Chariklia Georgopoulou. A Multi-Objective Metamodel-Assisted Memetic Algorithm with Strength-based Local Refinement. *Engineering Optimization*, 2009, 41 (10), pp.909-923. 10.1080/03052150902866577 . hal-00545364

**HAL Id: hal-00545364**

**<https://hal.science/hal-00545364>**

Submitted on 10 Dec 2010

**HAL** is a multi-disciplinary open access archive for the deposit and dissemination of scientific research documents, whether they are published or not. The documents may come from teaching and research institutions in France or abroad, or from public or private research centers.

L'archive ouverte pluridisciplinaire **HAL**, est destinée au dépôt et à la diffusion de documents scientifiques de niveau recherche, publiés ou non, émanant des établissements d'enseignement et de recherche français ou étrangers, des laboratoires publics ou privés.



## A Multi-Objective Metamodel-Assisted Memetic Algorithm with Strength-based Local Refinement

Journal:	<i>Engineering Optimization</i>
Manuscript ID:	GENO-2008-0182.R3
Manuscript Type:	Review
Date Submitted by the Author:	24-Feb-2009
Complete List of Authors:	Giannakoglou, Kyriakos; National technical University of Athens Georgopoulou, Chariklia; National Technical University of Athens
Keywords:	Metamodel-Assisted Memetic Algorithms, Fitness function, Strength, Multi-objective Optimization
Note: The following files were submitted by the author for peer review, but cannot be converted to PDF. You must view these files (e.g. movies) online.	
georgopoulou.tex georgopoulou_appendix.tex georgopoulou_figures.tex georgopoulou_macros.tex georgopoulou_tables.tex georgopoulou.bib	



## RESEARCH ARTICLE

## A Multi-Objective Metamodel-Assisted Memetic Algorithm with Strength-based Local Refinement

Chariklia A. Georgopoulou and Kyriakos C. Giannakoglou\*

National Technical University of Athens, School of Mechanical Engineering,  
Lab. of Thermal Turbomachines, Parallel CFD & Optimization Unit,  
P.O. Box 64069, Athens 157 10, Greece

(Received 00 Month 200x; final version received 00 Month 200x)

Metamodel-Assisted Evolutionary Algorithms are low-cost optimization methods for CPU demanding problems. Memetic Algorithms combine global and local search methods, aiming at improving the quality of promising solutions. This paper proposes a Metamodel-Assisted Memetic Algorithm which combines and extends the capabilities of the aforementioned techniques. Herein, metamodels undertake a dual role: they perform a low-cost pre-evaluation of population members during the global search and the gradient-based refinement of promising solutions. This reduces significantly the number of calls to the evaluation tool and overcomes the need for computing the objective function gradients.

In multi-objective problems, the selection of individuals for refinement is based on domination and distance criteria. During refinement, a scalar strength function is maximized and this proves to be beneficial in constrained optimization. The proposed Metamodel-Assisted Memetic Algorithm employs principles of Lamarckian learning and is demonstrated on mathematical and engineering applications.

**Keywords:** Metamodel-Assisted Memetic Algorithms; Fitness function; Strength; Multi-objective Optimization.

## 1. Introduction

In the literature, a considerable number of papers appeared on the use of surrogate evaluation models or metamodels to assist global search (*GS*) methods, Shan and Wang (2005), such as the Evolutionary Algorithms (*EAs*), Madsen *et al.* (2000), Ong *et al.* (2000), Ulmer *et al.* (2004, 2003), Jin *et al.* (2000), Buche *et al.* (2005), Lim *et al.* (2008). These

---

\*Corresponding author. Email: kgianna@central.ntua.gr

1  
2  
3  
4  
5 methods can be classified based on the way metamodels are coupled with or updated  
6 during the evolutionary search. Further discussion on the so-called Metamodel-Assisted  
7 Evolutionary Algorithms (*MAEAs*) can be found in relevant review papers and books  
8 such as in Giannakoglou (2002), Keane and Nair (2005), Jin *et al.* (2002). In *MAEAs*, the  
9 role of metamodels is to provide approximations to the fitness or cost of candidate solu-  
10 tions and, thus, save a great amount of evaluations which would otherwise be carried out  
11 by the CPU-demanding problem-specific tool. In Karakasis and Giannakoglou (2005),  
12 Giannakoglou *et al.* (2001), they are used to pre-evaluate the population members, in  
13 the so-called Inexact Pre-Evaluation (*IPE*) phase of each generation of the *MAEA*. *IPE*  
14 is based on metamodels trained on the fly, on a small number of already evaluated indi-  
15 viduals in the neighborhood of each individual (local metamodels).  
16

17 Memetic Algorithms (*MAs*), Dawkins (1976), Moscato (1999), Krasnogor (2002), Ong  
18 and Keane (2004), Ong *et al.* (2006), Krasnogor and Gustafson (2002), Hart (1994), are  
19 optimization methods that combine *GS* and local search (*LS*). *MAs* profit of the abilities  
20 of *EAs* to explore the most promising regions of the design space without being trapped  
21 into local optima and the efficiency of deterministic methods to further refine promising  
22 solutions located during *GS*. However, *MAs* may become CPU demanding, since they  
23 employ calls to the evaluation tool and, likely, the one computing the gradient of the  
24 objective function.  
25

26 This paper presents a Metamodel-Assisted Memetic Algorithm (*MAMA*) for multi-  
27 objective optimization (*MOO*) problems, in which locally trained metamodels approxi-  
28 mate the objective function values during the *GS* and the gradient required for the re-  
29 finement. The core *GS* tool is a *MAEA* whereas an ascent method, Nocedal and Wright  
30 (1999), using the gradient provided by the metamodels is used for the *LS*. The same  
31 set of patterns is used to train a radial basis function (*RBF*), Haykin (1999), network  
32 for each individual during the *IPE* phase of the *MAEA* and the refinement process. In  
33 contrast to the *MAEA* which, in *MOO* problems, seeks the Pareto set of non-dominated  
34 solutions, *LS* copes with the maximization of a (scalar) strength function. In the liter-  
35 ature of *MAs* for *MOO*, it is proposed either to refine only one of the objectives at a  
36 time, Bosman and de Jong (2005), or to handle a linear combination of weighted objec-  
37 tives, Ishibuchi and Murata (1996), Jaszkievicz (2002), Ishibuchi *et al.* (2003), Lim *et al.*  
38 (2008). The *MPAES* algorithm proposed in Knowles and Corne (2000) is an exception  
39 since it employs a form of Pareto ranking based on comparing individuals to an archive  
40 of non-dominated solutions.  
41

42 In the present paper, a new scheme is proposed. The function to be maximized in *LS*  
43 is a strength function that takes into account domination criteria. During the refinement  
44 process, the local *RBF* networks are re-trained on the strength function values, com-  
45 puted by considering the current offspring, parent and elite populations, and are used to  
46 compute ascent directions. This is important when the objective functions have rugged  
47 landscapes or we are dealing with constrained problems where the objective function is  
48 penalized proportionally to the degree of constraints' violation. The outcome of the *LS*  
49 process may displace the starting point, for both genotype and phenotype, according to  
50 the Lamarckian learning rules. Relevant papers on *MAMAs* almost exclusively focus on  
51 single-objective optimization (*SOO*) problems and make use of metamodels to support  
52 either both *GS* and *LS*, Zhou *et al.* (2007a,b), or only *LS*, Liang *et al.* (1999, 2000),  
53 Hacker (2002).  
54

55 The proposed *MAMA* is firstly demonstrated on mathematical benchmark cases and  
56 its performance is analyzed statistically and compared to *EAs* and *MAEAs*. Two con-  
57 strained engineering applications, namely the design of a combined cycle power plant and  
58  
59  
60

a compressor cascade, are also studied. All the examined cases deal with two objectives.

## 2. The Proposed MAMA

The proposed MAMA was built on an existing MAEA, Giannakoglou (2002), for MOO problems with  $M$  objectives. One may clearly distinguish the proposed MAMA from a MAEA or a “conventional” MA by (a) the LS algorithm which relies on local metamodells trained on a scalar strength function to be maximized and (b) the coupling of LS with the core MAEA, where a scheme for selecting individuals for LS is proposed.

MAMA involves four sets of candidate solutions: the offspring set  $\mathcal{P}_{\lambda,g}$ , the parent set  $\mathcal{P}_{\mu,g}$ , the archival set  $\mathcal{P}_{\alpha,g}$  (which progressively approaches the Pareto front of non-dominated solutions) and an extra set  $\mathcal{P}_{LS,g}$  of individuals qualified to undergo LS. The second index  $g$  stands for the generation counter. Candidate solutions are denoted by  $\vec{x} \in \mathcal{R}^N$  and the objective function vector is  $\vec{F}(\vec{x}) \in \mathcal{R}^M$ . During the first few generations ( $g < g^{IPE}$ , where  $g^{IPE}$  is user-defined), the proposed MAMA behaves as a  $(\mu, \lambda)$  EA and the  $\lambda$  offspring are all evaluated on the problem-specific tool. The so-evaluated individuals  $\vec{x}$ , paired with the  $\vec{F}(\vec{x})$  values, are recorded in a database  $\mathcal{D}$ .

Dealing with MOO problems, it is necessary to adopt a fitness assignment technique; through this technique a unique scalar fitness value  $\phi$  is assigned to each population member, depending on its  $\vec{F}(\vec{x})$  and dominance criteria. Herein, the selected technique was inspired by the widely used SPEA2 (Strength Pareto EA), Zitzler *et al.* (2001). Two terms contribute additively to the fitness value  $\phi$  of any individual. The first term is the raw fitness  $R$  and the second is density  $D$ . The raw fitness  $R$  of an individual is determined by the strength  $S$  (i.e. the number of dominated individuals) of its dominators in  $\mathcal{P}_{\lambda,g}$ . The  $D$  value of each individual is determined by its distance from the  $k$ th closest neighbor in the normalized objectives space, where  $k = \sqrt{\lambda}$ . Then the scalar  $\phi = \phi(R(S), D)$  value is computed, as in Zitzler *et al.* (2001). An illustrative example of the calculation of  $\phi$  is shown in figure 1. In the sake of clarity, when  $\phi$  is computed using approximate objective function values  $\tilde{\vec{F}}(\vec{x})$  (provided by the metamodells during the IPE phase, see Step 1 below), this will be denoted by  $\tilde{\phi}$ .

The MAMA steps presented below apply if  $g \geq g^{IPE}$ , during which  $\mathcal{D}$  is non-empty ( $|\mathcal{D}| = \lambda_{\mathcal{D}}$ ) and continues to be updated by recording all new individuals evaluated on the problem-specific tool. In figure 3, the corresponding algorithm flowchart is shown.

- Step 1. [GS: Inexact Pre-Evaluations] For each individual  $\vec{x} \in \mathcal{P}_{\lambda,g}$ , its  $K$  closest  $\mathcal{D}$  entries are selected to populate the corresponding training set  $\mathcal{T}_K$ . It is recommended that  $K$  takes on a value close to (or slightly higher than) the number  $N$  of design variables. An RBF network (with  $N$  input and  $M$  output units;  $N$  and  $M$  are equal to the number of design variables and the number of objectives, respectively) is trained on the objective function vectors of the  $\mathcal{T}_K$  patterns and an approximate  $\tilde{\vec{F}}(\vec{x})$  is obtained. After the metamodel-based evaluation (for all but the  $\mathcal{P}_{\lambda,g}$  members which have been previously evaluated and can be restored from  $\mathcal{D}$ ) and by applying dominance and strength criteria, as previously described, fitness values  $\phi$  and  $\tilde{\phi}$  are assigned to all individuals in  $\mathcal{P}_{\lambda,g}$ . The  $\lambda$  individuals are sorted according to their fitness values (irrespective of the evaluation tool used) and the top  $\lambda_e$  of them are selected to populate  $\mathcal{P}_{e,g}$ , where  $\lambda_e < \lambda$  is a user-defined integer.
- Step 2: [GS: Exact evaluations] Each  $\vec{x} \in \mathcal{P}_{e,g}$  is re-evaluated using the problem-specific tool and stored in  $\mathcal{D}$ . The  $\vec{F}(\vec{x})$  values displace the metamodel-based ones for the

$\mathcal{P}_{e,g}$  members. In constrained optimization cases, if a candidate solution violates even a single constraint, the corresponding  $\vec{F}(\vec{x})$  includes an exponential penalty factor depending on the degree of constraint violation.

Step 3. [LS: Preparation] A number of  $\mathcal{P}_{\lambda,g}$  members for which  $\vec{F}(\vec{x})$  are known, is singled out in  $\mathcal{P}_{LS,g}$  ( $\lambda_{LS} = |\mathcal{P}_{LS,g}|$ ), according to distance and dominance criteria, as it will be discussed elsewhere in this paper. The  $\mathcal{P}_{LS,g}$  members are selected from  $\mathcal{P}_{e,g}$  ( $\subset \mathcal{P}_{\lambda,g}$ ) and the subset  $\mathcal{P}_{\lambda,g} \cap \mathcal{D}$ , so that only individuals that have been evaluated on the problem-specific tool may undergo LS.

Step 4. [LS: Refinement] The previously populated  $\mathcal{P}_{LS,g}$  members are refined using a gradient-based descent method which, in contrast to conventional MAs, aims at maximizing their strength  $S$ . This search is subject to  $2N$  inequality constraints, corresponding to the upper and lower variables' bounds. To avoid calculations on the problem-specific tool during LS, the gradient of  $S$  is approximated using the RBF network trained on the  $S$  values of the  $\mathcal{T}_K$  patterns associated with each individual (as formed in Step 1). The process initiates from the genotype  $\vec{x}$  of the individual for which both  $\vec{F}(\vec{x})$  (from Step 2) and strength  $S$  (from Step 3) are known and ends up with a new individual  $\vec{x}^*$ . This should be evaluated on the problem-specific tool before being accepted or not. The new individual is archived in  $\mathcal{D}$  and, in case the starting objectives vector is improved, both  $\vec{x}^*$  and  $\vec{F}(\vec{x}^*)$  displace  $\vec{x}$  and  $\vec{F}(\vec{x})$  in  $\mathcal{P}_{\lambda,g}$  and  $\mathcal{P}_{LS,g}$  according to the Lamarckian learning rules. An example of the LS process is shown in figure 2.

Step 5. [GS: Evolution] Fitness  $\phi$  and  $\tilde{\phi}$  are updated for all individuals in  $\mathcal{P}_g = \mathcal{P}_{\mu,g} \cup \mathcal{P}_{\lambda,g} \cup \mathcal{P}_{\alpha,g}$ . The elitism operator  $E$  is applied to  $\mathcal{P}_{e,g}$  and  $\mathcal{P}_{\alpha,g}$  to update the elite set and the evolution operators (parent selection  $P$ , crossover  $C$  and mutation  $M$ ) to create the new offspring population. Schematically,

$$\mathcal{P}_{e,g+1} = E(\mathcal{P}_{e,g} \cup \mathcal{P}_{\alpha,g})$$

$$\mathcal{P}_{\mu,g+1} = P(\mathcal{P}_{\mu,g} \cup \mathcal{P}_{\lambda,g})$$

$$\mathcal{P}_{\lambda,g+1} = M(C(\mathcal{P}_{\mu,g+1}, \mathcal{P}_{\alpha,g+1})).$$

Step 6. [Termination] If the maximum number of evaluations (on the problem-specific tool) is reached or the set  $\mathcal{P}_{\alpha}$  remains unchanged for a number of generations, the algorithm terminates. Otherwise,  $g \leftarrow g+1$  and the evolution continues from Step 1.

As already discussed, in order to maximize the expected gain from the refinement process,  $\mathcal{P}_{LS,g}$  should be carefully populated. The number of refined individuals  $\lambda_{LS}$  is not fixed and the user defines only its upper bound  $\lambda_{LS}^{max}$ . In MOO problems, LS should hopefully give new solutions that either dominate one or more members of the current archival front or fill the gap between two non-dominated members or stretch the current front. In problems with multimodal objective functions, it is evident that whether a gradient-based search may or may not achieve any of these goals depends on the starting point. Thus, the formation of  $\mathcal{P}_{LS,g}$  is based on three selection rules:

- $\mathcal{P}_{LS,g}$  is populated by individuals evaluated on the problem-specific tool.
- Candidates with higher strength  $S$  must be selected with priority;  $S$  is calculated by processing  $\mathcal{P}_{\lambda,g}$  without taking into consideration the evaluation tool (problem-specific tool or metamodel).
- A candidate is not allowed to enter  $\mathcal{P}_{LS,g}$  if it lies in the vicinity of a previous entry.

To summarize, among neighboring candidates, the most dominant one is chosen and the

1  
2  
3  
4  
5 others are excluded. For instance, consider that among the two neighboring candidate  
6 solutions  $A$  and  $B$  shown with circles in figure 4, only one must be selected for  $LS$ .  
7 Though  $A$  does not dominate  $B$  and vice-versa,  $A$  is selected for  $LS$  since its strength is  
8 higher.  
9

### 10 11 12 3. Method Application & Assessment

#### 13 14 3.1. Validation on Mathematical Problems

15 Before going through the two engineering applications, a thorough validation of the  
16 proposed method on three two-objective function minimization problems is presented in  
17 brief. These problems are known as the  $ZDT1$ ,  $ZDT2$  and  $ZDT3$  (see Zitzler *et al.* (2000)  
18 for detailed descriptions) and correspond to convex, concave and discontinuous Pareto  
19 fronts, respectively. Each of them involved 30 optimization variables and was solved using  
20  $EA$ ,  $MAEA$  and the proposed  $MAMA$ . To cope with  $MOO$  problems, the  $SPEA2$  fitness  
21 assignment algorithm was used in all of them. Each run was repeated 25 times with  
22 different random number generation (RNG) seeds. The statistical processing of results  
23 is based on the hypervolume performance indicator  $I_H$ , Huang *et al.* (2007). Using  $I_H$ ,  
24 the front quality is quantified by the percentage of the volume (area) of a bounding box  
25 which is not dominated by the front. By definition, small  $I_H$  values denote high quality  
26 fronts.  
27

28  
29 For all optimization runs, the parent and offspring populations used in  $EA$ ,  $MAMA$   
30 and  $MAEA$  had  $\mu=60$  and  $\lambda=100$  members, respectively. For the  $MAEA$  and  $MAMA$ ,  
31 the  $IPE$  phase (i.e. the use of metamodels) started when the database  $\mathcal{D}$  (of previously  
32 evaluated individuals) size exceeded 400 ( $\lambda_{\mathcal{D}} \geq 400$ ). In  $MAMA$ , the  $LS$  started simulta-  
33 neously with the  $IPE$  phase. Also, at each generation  $\lambda_e=15$  and  $\lambda_{LS}^{max}=12$ .  
34

35 Tables 1, 2 and 3 present statistical measures of the performances of the three algo-  
36 rithms during the evolution and demonstrate the superiority of  $MAMA$ , compared to  
37  $MAEA$  and  $EA$ . Statistical t-tests on the average  $I_H$  values prove that, with the same  
38 CPU cost,  $MAMA$  outperforms  $EA$  and  $MAEA$  for a confidence level of 99.9% and for  
39 all the tested problems. Table 4 shows the outcomes of the t-test analysis of the  $ZDT3$   
40 results. The reader may also refer to figures 5, 6 and 7 for a visual comparison of the opti-  
41 mal fronts obtained at the same CPU cost. Note that, in all cases, more than 60% of the  
42 individuals selected for  $LS$  were improved at least with respect to one of the objectives.  
43  
44

#### 45 46 3.2. Design of a Combined Cycle Power Plant

47 This application is concerned with the optimal design of a combined cycle power plant  
48 ( $CCPP$ , Bonataki *et al.* (2004)). The power plant consists of a gas turbine ( $GT$ ) produc-  
49 ing a power output of 120 MW, a dual-pressure heat recovery steam generator ( $HRSG$ ), a  
50 two-admission steam turbine ( $ST$ ), feedwater tank, condenser, condensate and feedwater  
51 pumps and two generators ( $G_1$  and  $G_2$ ), as in figure 8. At the exit of the  $GT$ , the flue  
52 gas is cooled by traversing seven high- and low-pressure heat exchangers in the  $HRSG$ .  
53 Superheated high- and low-pressure steam is generated which is, then, expanded in the  
54  $ST$ .  
55

56 The 13 design parameters in total are classified to those determining the  $GT$  per-  
57 formance (pressure ratio, air-to-fuel ratio, polytropic efficiencies of the compressor and  
58 turbine, etc.) and those related to the  $HRSG$  design variables (heat exchange areas,  
59  
60

operating pressures and temperatures for the working fluids).

In the present design, the two objectives to be maximized were the power plant efficiency and the produced power. The design was subject to a number of constraints related among other to the requirement that flue gas temperatures should exceed the water or steam temperature (by a safety margin) at different points along the *HRSG*. Due to the high number of constraints, many heavily penalized individuals entered  $\mathcal{D}$  and this might cause troubles if the *RBF* networks were trained on penalized responses. For example, to approximate the score of a feasible solution which, in the design space, is located close to even a single infeasible solution, the presence of the latter in the *RBF* network training set may heavily mislead its prediction. The situation may become even worse, if the same *RBF* network was also used to drive *LS*. This problem is alleviated since the *RBF* network that supports *LS* is trained on the strength function values  $S$  instead of the penalized cost values. This is a noticeable advantage of the proposed *MAMA*.

As in the previous cases, the proposed *MAMA* is compared with *MAEAs* and *EAs*, based on three individual runs (using different RNG seeds). The core  $(\mu, \lambda)$ -EA used in *MAMA* and *MAEA* had a common configuration:  $\mu = 40$ ,  $\lambda = 60$ ; *LS* and the *IPE* phase initiated when  $\lambda_{\mathcal{D}} \geq 400$ . Also,  $\lambda_e = 15$ ,  $\lambda_{LS}^{max} = 10$ .

Average  $I_H$  indicator values and the range of deviation around the mean for a 66% probability are shown in figure 9. A t-test analysis on the final results (for 10000 exact evaluations) proved that, for 99.9% probability and irrespective of the RNG seed, *MAMA* reaches better optimal fronts than *EA* or *MAEA* (*MAMA* vs. *EA*:  $t_0 = 13.03$  and *MAMA* vs. *MAEA*:  $t_0 = 3.42$ ).

Figure 10 presents the fronts of non-dominated solutions obtained using the three algorithms at the cost of 500, 3000, 7000 and 10000 exact evaluations, for one of the three RNG seeds. It is obvious that *MAMA* performs better than the other two algorithms. In figure 11, some statistics on the performance of the *LS* process are shown; during the evolution, an average percentage of 45% of the members in  $\mathcal{P}_{LS}$  were improved by *LS*, for at least one of the objectives.

### 3.3. Two Operating Point Optimization of a Compressor Cascade Airfoil

The second engineering test case is concerned with the design of an optimal compressor cascade airfoil at two operating points, with two objectives. The first objective is the minimization of the total pressure loss coefficient  $\omega$  at the design point  $OP_1$  (inlet flow angle  $\alpha_1^{(OP_1)} = 47^\circ$ , inlet Mach number  $M_1^{(OP_1)} = 0.618$  and Reynolds  $R_e^{(OP_1)} = 8.41 \cdot 10^5$ ). The second objective is the minimization of the same quantities at a different operation point  $OP_2$  ( $\alpha_1^{(OP_2)} = 52^\circ$ ,  $M_1^{(OP_2)} = 0.621$  and  $R_e^{(OP_2)} = 7.63 \cdot 10^5$ ). The cascade streamtube thickness before the leading edge (*LE*) and after the trailing edge (*TE*) was fixed to 1.0 and  $\sim 0.9$ , respectively, Axial-Velocity-Density-Ratio with a linear variation in between *LE* and *TE* ( $AVDR = \sim 0.9$ ).

The objective function to be minimized was expressed by  $\omega = \frac{p_{t2, is} - p_{t2}}{p_{t1} - p_1}$ , where  $p$  and  $p_t$  stand for static and total pressure, the subscripts 1 and 2 correspond to the cascade inlet and exit and *is* denotes isentropic flow. Drela's *MISES* analysis software for cascades, Drela and Giles (1987), was used for the evaluation of candidate airfoils during the optimization. *MISES* is based on an integral boundary layer method coupled with an external inviscid flow solver.

All candidate designs were subject to geometrical and flow constraints, related to



1  
2  
3  
4  
5 the airfoil thickness (not allowed to exceed some minimum values at several chordwise  
6 positions) and the flow turning (which should exceed  $\Delta\alpha_{12}^{(OP_1)} = 24^\circ$  and  $\Delta\alpha_{12}^{(OP_2)} = 27^\circ$ ).

7 The airfoil pressure and suction sides were parameterized using two Bezier polynomial  
8 curves, with 7 control points each, giving rise to 20 design variables in total. On both  
9 curves, the first and last control points were kept fixed whereas the remaining five control  
10 points were free to vary within user-defined bounds.

11 The optimization was carried out by implementing a core  $(\mu, \lambda)$ -EA (20,40) for all  
12 algorithms (*EA*, *MAEA* and *MAMA*); *LS* and *IPE* phase started at  $\lambda_D = 300$ , with  
13  $\lambda_e = 8$  and  $\lambda_{LS}^{max} = 4$ .

14 Figure 12 illustrates the non-dominated front computed by the three algorithms at the  
15 same cost of 5000 calls to the *MISES* software and the “convergence” history expressed in  
16 terms of the hypervolume indicator  $I_H$ . Note that, during the first 1000 evaluations, the  
17 two metamodel-assisted algorithms showed an equally efficient performance, compared  
18 to *EAs*. After 1500 evaluations, *MAMA* descended further though *MAEAs* and *EAs*  
19 drifted slowly without noticeable improvement in  $I_H$ . The elite front resulted from the  
20 *MAMA* after 5000 evaluations outperforms all the rest. For the optimal front computed  
21 by *MAMA* shown in figure 12 (right), its edge points were post-processed and are shown  
22 in figure 13 (contour profiles, isentropic Mach number distribution along the airfoil).  
23  
24  
25  
26  
27

#### 28 4. Conclusions – Comments

29  
30 This paper presents a Metamodel-Assisted Memetic Algorithm which is suitable for  
31 multi-objective, constrained optimization problems. The proposed *MAMA* is advanta-  
32 geous since, as shown in the examined cases, reduces the CPU cost compared to conven-  
33 tional *MAs* or *MAEAs*. It was beyond the scope of this paper to compare this population-  
34 based stochastic algorithm with any other deterministic search algorithm. Such a compar-  
35 ison would simply come up with the well-known differences in efficiency and effectiveness  
36 of the two “rival” classes of methods. The purpose of this paper was to demonstrate the  
37 *MAMAs* superiority with respect to two methods (*EAs* and *MAEAs*) of the same class.

38 The CPU reduction was achieved by implementing local metamodels, trained on the  
39 fly on a small number of neighboring individuals, separately for each new candidate  
40 solution. The metamodels support both global and local search. During the local search,  
41 a novelty of our method is that the metamodel training is based on strength values  
42 (scalars that represent the number of offspring dominated by an individual) rather than  
43 objective function values. In constrained problems, where the objective function might  
44 be penalized due to the violation of constraints and/or problems where the objective  
45 function has a rugged landscape, this is important since penalties or abrupt landscape  
46 slopes do not affect the metamodel predictions.  
47  
48

49 We have chosen to use *RBF* networks which often produce better fits to various types  
50 of functions, compared to other rival techniques (such as polynomial regression or the  
51 kriging metamodel; see Jin and Chen (2001)); however, any other metamodel can be  
52 used instead. Depending on the problem, gradients computed using the *RBF* networks  
53 may be inaccurate but this doesn't affect the good performance of our method. This is  
54 attributed to two key features of our method (a) each *RBF* network corresponds to a  
55 small part of the search space, where the landscape is not usually expected to be rugged  
56 enough and (b) the landscape modeled by networks is the strength function. Therefore,  
57 to the authors' experience, inaccurate predictions of the strength gradient from the *RBF*  
58 network, during the local refinements, is not risky. According to the results shown here  
59  
60

1  
2  
3  
4  
5 as well as other applications studied using this method, this neither imposes limitations  
6 to the applicability of the proposed method nor increases its CPU cost (due to the fact  
7 that during each refinement, either successful or failed due to *RBF* network inaccuracies,  
8 the extra CPU cost is that of a single evaluation).  
9

## 10 11 12 5. Acknowledgment

13  
14 This work was co-funded by the PENED03 program (Measure 8.3 of the Operational  
15 Program Competitiveness, of which 80 % is European Commission and 20 % national  
16 funding), under project number 03ED111.  
17

## 18 19 20 References

- 21  
22 Bonataki, E., Georgoulis, L., and Giannakoglou, C.G.K.C., 2004. Optimal design of com-  
23 bined cycle power plants based on gas turbine performance data. *In: ERCOFTAC*  
24 *Design Optimization: Methods & Applications*, Athens, Greece, 31 March - 2 April  
25 2004., Athens.
- 26  
27 Bosman, A. and de Jong, D.E., 2005. Exploiting gradient information in numerical  
28 multi-objective evolutionary optimization. *In: GECCO '05: Genetic and Evolution-*  
29 *ary Computation Conference*, Washington DC, USA New York, NY, USA: ACM,  
30 755–762.
- 31  
32 Buche, D., Schraudolph, N.N., and Koumoutsakos, P., 2005. Accelerating evolutionary  
33 algorithms with gaussian process fitness function models. *IEEE Transactions on*  
34 *Systems, Man and Cybernetics – Part C: Applications and Reviews*, 35, 183–194.
- 35  
36 Dawkins, R., 1976. *The selfish gene*. Oxford: Oxford University Press.
- 37  
38 Drela, M. and Giles, M., 1987. Viscous-inviscid analysis of transonic and low Reynolds  
39 number airfoils. *AIAA Journal*, 25 (10), 1347–1355.
- 40  
41 Giannakoglou, K., Giotis, A., and Karakasis, M., 2001. Low-Cost Genetic Optimization  
42 based on Inexact Pre-Evaluations and the Sensitivity Analysis of design parameters.  
43 *Journal of Inverse Problems in Engineering*, 9 (4), 389–412.
- 44  
45 Giannakoglou, K.C., 2002. Viscous-inviscid analysis of transonic and low Reynolds num-  
46 ber airfoils. *International Review Journal Progress in Aerospace Sciences*, 38, 43–7  
47 6.
- 48  
49 Hacker, K., 2002. Efficient global optimization using hybrid genetic algorithms. *In: 9th*  
50 *AIAA//ISSMO: Symposium on Multidisciplinary Analysis and Optimization*, At-  
51 lanta, USA.
- 52  
53 Hart, W., 1994. Adaptive Global Optimization with Local Search. Thesis (PhD). Uni-  
54 versity of California, USA.
- 55  
56 Haykin, S., 1999. *Neural networks: A comprehensive foundation*. Prentice Hall Interna-  
57 tional, Inc.
- 58  
59 Huang, V.L., *et al.*, Problem Definitions for Performance Assessment of Multi-objective  
60 Optimization Algorithms. , 2007. , Technical report, Nanyang Technological Univer-  
sity, Singapore Special Session on Constrained Real-Parameter Optimization.
- Ishibuchi, H. and Murata, T., 1996. Multiobjective genetic local search algorithm. *In:*  
*IEEE International Conference on Evolutionary Computation*, Nagoya, Japan, 20-22  
May 1996., 119–124.
- Ishibuchi, H., Yoshida, T., and Murata, T., 2003. Balance between genetic search and

- 1  
2  
3  
4  
5 local search in memetic algorithms for multiobjective permutation flowshop schedul-  
6 ing. *IEEE Transactions on Evolutionary Computation*, 7 (2), 204–223.
- 7 Jaszkiwicz, A., 2002. Genetic local search for multi-objective combinatorial optimiza-  
8 tion. *European Journal of Operational Research*, 137 (22), 50–71.
- 9 Jin, R. and Chen, W., 2001. Comparative studies of metamodeling techniques under  
10 multiple modeling criteria. *Structural and Multidisciplinary Optimization*, 23, 1–13.
- 11 Jin, Y., Olhofer, M., and Sendhoff, B., 2000. On evolutionary optimization with approx-  
12 imate fitness functions. In: D.W. et al., ed. *GECCO '00: Genetic and Evolutionary  
13 Computation Conference* Morgan Kaufmann, 786–793.
- 14 Jin, Y., Olhofer, M., and Sendhoff, B., 2002. A Framework for Evolutionary Optimization  
15 With Approximate Fitness Functions. *IEEE Transactions on Evolutionary Compu-  
16 tation*, 6 (5), 481–494.
- 17  
18 Karakasis, M. and Giannakoglou, K., 2005. On the use of metamodel-assisted, multi-  
19 objective evolutionary algorithms. *Engineering Optimization*, 38 (8), 941–957.
- 20 Keane, A. and Nair, P., 2005. *Computational approaches for aerospace design: The  
21 pursuit of excellence*. West Sussex: John Wiley & Sons, Inc.
- 22 Knowles, J. and Corne, D., 2000. M-PAES: A memetic algorithm for multiobjective  
23 optimization. In: *2000 Congress on Evolutionary Computation – CEC '00* IEEE  
24 Press, 325–332.
- 25 Krasnogor, N., 2002. Studies on the theory and design space of memetic algorithms.  
26 Thesis (PhD). UK.
- 27 Krasnogor, N. and Gustafson, S., 2002. Toward truly "memetic" memetic algorithms:  
28 discussion and proof of concepts. In: *Advances in Nature-Inspired Computation: The  
29 PPSN VII Workshops. PEDAL (Parallel, Emergent and Distributed Architectures  
30 Lab)*. University of Reading. ISBN 0-9543481-0-9. *icalp.tex; 9/12/2003; 16:52; p.21  
31 22 Natalio Krasnogor, Steven Gustafson*.
- 32  
33 Liang, K., Yao, X., and Newton, C., 1999. Combining landscape approximation and local  
34 search in global optimization. In: *CEC '99, Congress on Evolutionary Computation*,  
35 Washington, USA IEEE Press, 1514–1520.
- 36 Liang, K., Yao, X., and Newton, C., 2000. Evolutionary search of approximated n-  
37 dimensional landscapes. *International Journal of Knowledge-based Intelligent En-  
38 gineering Systems*, 4, 172–183.
- 39 Lim, D., et al., 2008. Generalizing surrogate-assisted evolutionary computation. *IEEE  
40 Transactions on Evolutionary Computation*, in press.
- 41 Madsen, J., Shyy, W., and Haftka, R., 2000. Response Surface Techniques for Diffuser  
42 Shape Optimization. *AIAA Journal*, 38, 1512–1518.
- 43 Moscato, P., 1999. *Memetic algorithms: A short introduction*. McGraw-Hill Company.
- 44 Nocedal, J. and Wright, S.J., 1999. *Numerical Optimization*. Springer-Verlag.
- 45 Ong, Y.S., et al., 2006. Classification of adaptive memetic algorithms: a comparative  
46 study. *IEEE Transactions on Systems, Man, and Cybernetics – Part B*, 36 (1), 141–  
47 152.
- 48 Ong, Y. and Keane, A., 2004. Meta-Lamarckian learning in memetic algorithms. *Evolu-  
49 tionary Computation*, *IEEE Transactions on*, 8 (2), 99–110.
- 50 Ong, Y., Nair, P., and Keane, A., 2000. Evolutionary Optimization of Computationally  
51 Expensive Problems via Surrogate Modeling. *AIAA Journal*, 41 (4), 687–696.
- 52 Shan, S. and Wang, G.G., 2005. An Efficient Pareto Set Identification Approach for  
53 Multiobjective Optimization on Black-Box Functions. *Journal of Mechanical Design*,  
54 127 (5), 866–874.
- 55  
56 Ulmer, H., Streichert, F., and Zell, A., 2003. Model-assisted steady-state evolution strate-  
57  
58  
59  
60

- gies. In: *GECCO '03: Genetic and Evolutionary Computation Conference*, Chicago, USA, Chicago, USA, 610–621.
- Ulmer, H., Streichert, F., and Zell, A., 2004. Evolution strategies with controlled model assistance. In: *CEC '04, Congress on Evolutionary Computation*, Portland, USA, Portland, USA.
- Zhou, Z., *et al.*, 2007a. Memetic algorithm using multi-surrogates for computationally expensive optimization problems. *Journal of Soft Computing*, 11 (10), 957–971.
- Zhou, Z., *et al.*, 2007b. Combining global and local surrogate models to accelerate evolutionary optimization. *IEEE Transactions on Systems, Man, and Cybernetics – Part C: Applications and Reviews*, 37 (1), 66–76.
- Zitzler, E., Deb, K., and Thiele, L., 2000. Comparison of multiobjective evolutionary algorithms: empirical results. *Evolutionary Computation*, 8, 173–195.
- Zitzler, E., Laumans, M., and Thiele, L., SPEA2: Improving the Strength Pareto Evolutionary Algorithm for multiobjective optimization. , 2001. , Technical report, Zurich TIK-Report 103.

## 6. Appendix

For the validation of the proposed method, three benchmark two-objective function minimization problems, namely the *ZDT1*, *ZDT2* and *ZDT3* (see Zitzler *et al.* (2000)) test problems, were solved. For all the *ZDT*-problems, the equations expressing the design space and the objective functions are given in equations 1 and 2. The functions  $G(\vec{x})$  and  $h(\vec{x})$  differ among the three test cases.

$$F_1(\vec{x}) = x_1 \quad \text{and} \quad F_2(\vec{x}) = h(\vec{x})G(\vec{x}) \quad (1)$$

$$\vec{x} \in \mathcal{R}^N, \quad N = 30, \quad x_n \in [0, 1], \quad n = 1, N \quad (2)$$

The *ZDT1* problem has a convex optimal Pareto front, shown in the upper-left plot in figure 14. The functions  $G(\vec{x})$  and  $h(\vec{x})$  are given in equation 3.

$$G(\vec{x}) = 1 + \frac{9}{N-1} \sum_{n=2}^N x_n, \quad h(\vec{x}) = 1 - \sqrt{\frac{F_1(\vec{x})}{G(\vec{x})}} \quad (3)$$

The *ZDT2* problem has a concave optimal Pareto front, shown in figure 14, upper-right. The functions  $G(\vec{x})$  and  $h(\vec{x})$  are given in equation 4

$$G(\vec{x}) = 1 + \frac{9}{N-1} \sum_{n=2}^N x_n, \quad h(\vec{x}) = 1 - \left(\frac{F_1(\vec{x})}{G(\vec{x})}\right)^2 \quad (4)$$

*ZDT3* leads to a discontinuous Pareto front shown in the lower plot in figure 14, achieved by setting  $x_n = 0$ ,  $n = 2, N$ . The functions  $G(\vec{x})$  and  $h(\vec{x})$  are given in equation 5.

$$G(\vec{x}) = 1 + \frac{9}{N-1} \sum_{n=2}^N x_n, \quad H(\vec{x}) = 1 - \sqrt{\frac{F_1(\vec{x})}{G(\vec{x})} - \frac{F_1(\vec{x})}{G(\vec{x})} \sin(10\pi F_1(\vec{x}))} \quad (5)$$

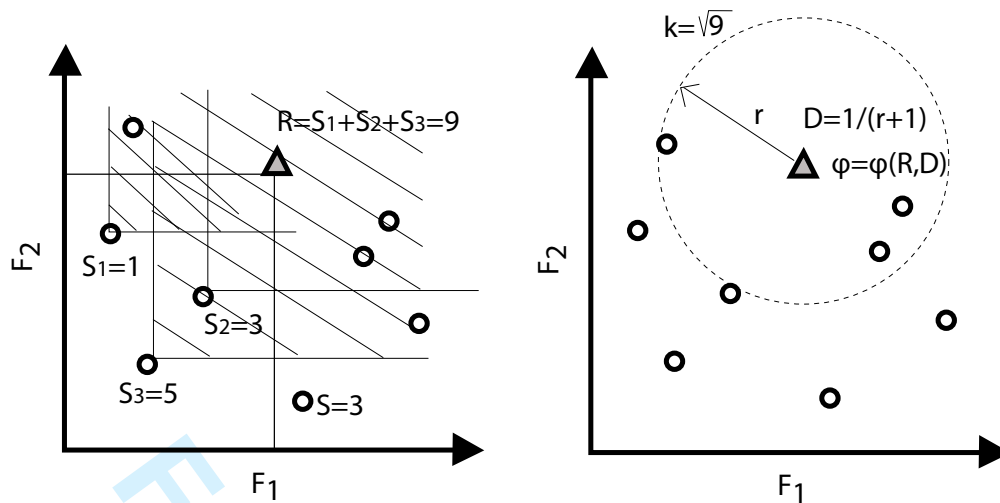


Figure 1. Calculation of the fitness  $\phi$  for MOO cases, according to the raw fitness  $R$ , the strength  $S$  and the density  $D$ . The strength  $S$  of any individual equals the number of the rest members in  $\mathcal{P}_\lambda$  it dominates. For the individual shown with a triangle, its  $R$  value is determined by the summation of strengths of its dominators, i.e.  $R = S_1 + S_2 + S_3$ . Its density  $D$  is adversely proportional to the distance from its closest  $\sqrt{\lambda}$  neighbor in the objectives space. Finally, its fitness  $\phi$  equals the summation of  $R$  plus  $D$ . For further details on the  $\phi$  function, the reader is addressed to Zitzler *et al.* (2001).

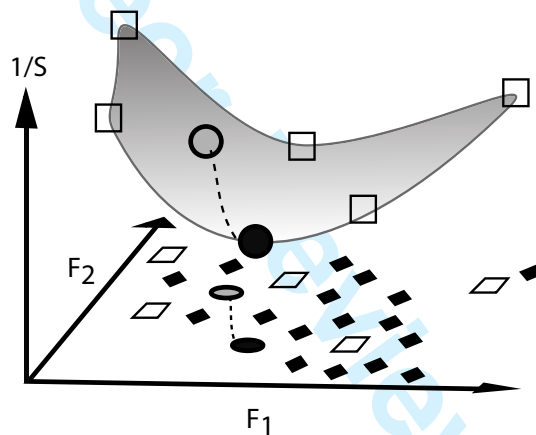


Figure 2. Example of the LS process. Training patterns are marked with empty squares. The individual to be refined is marked with the empty circle and the LS outcome with a black filled circle. Black diamonds correspond to the offspring population.

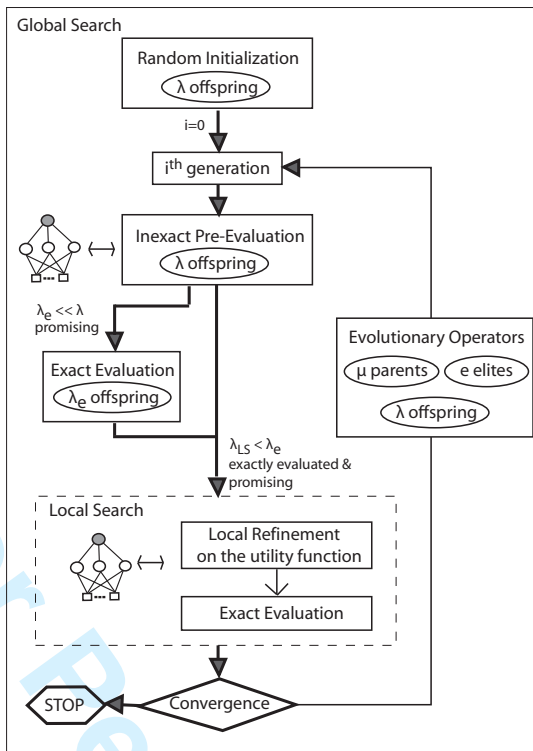


Figure 3. Flowchart of the proposed *MAMA* algorithm.

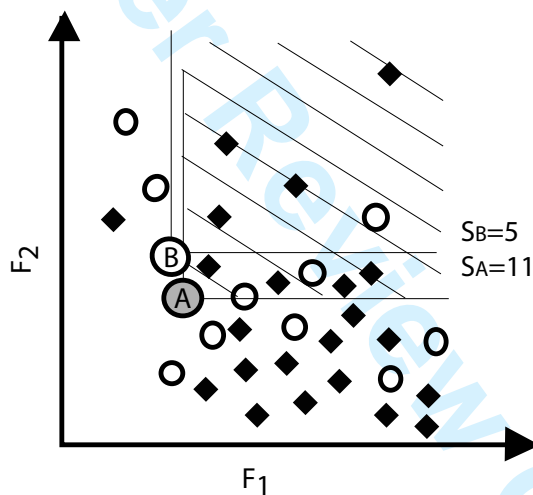


Figure 4. Example of the selection of individuals to undergo refinement. Individuals with circles represent individuals evaluated on the problem-specific tool ( $\mathcal{P}_{e,g}$ ), whereas diamonds correspond to offspring ( $\mathcal{P}_{\lambda,g} \setminus \mathcal{P}_{e,g}$ ) evaluated only on the metamodel. Among *A* and *B*, *A* is the most favored to be selected for *LS*, since its strength is greater than the one of *B* and, thus, its refinement is more likely to lead to improvement.

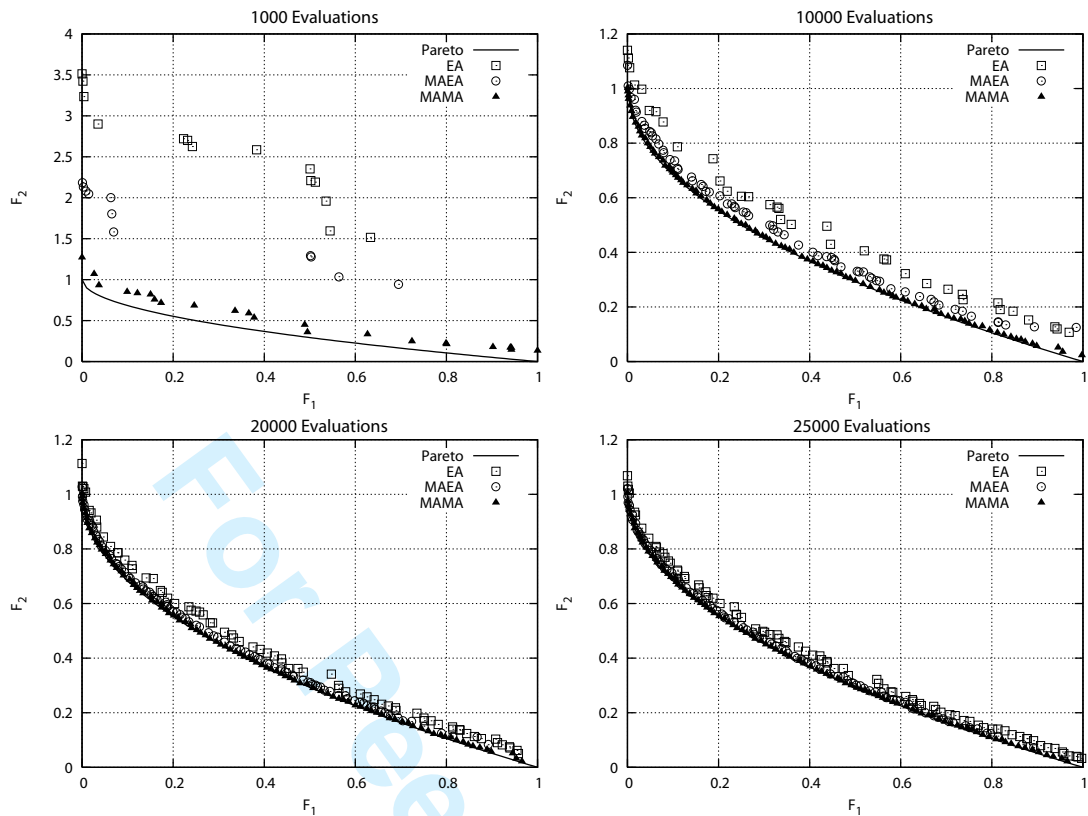


Figure 5. *ZDT1*: Fronts of the elite solutions for *EA*, *MAEA*, *MAMA* at the cost of 1000 (top-left), 10000 (top-right), 20000 (bottom-left) and 25000 (bottom-right) calls to the function evaluation tool for the best performing RNG seed. The exact Pareto front corresponds to the continuous line.

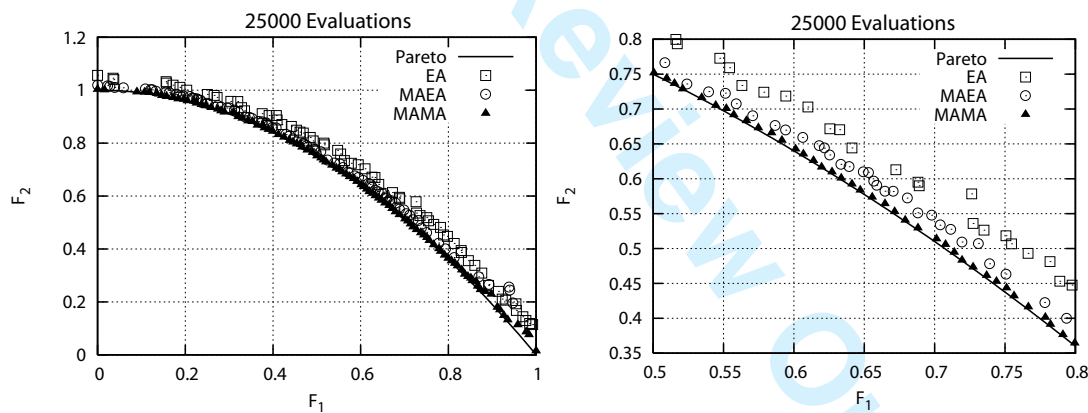


Figure 6. *ZDT2*: Fronts of the elite solutions for *EA*, *MAEA*, *MAMA* at the cost of 25000 (left) calls to the function evaluation tool for the best performing RNG seed. The right plot focuses on a part of the optimal front, to clearly show that the proposed *MAMA* approximates better the exact Pareto front (continuous line).



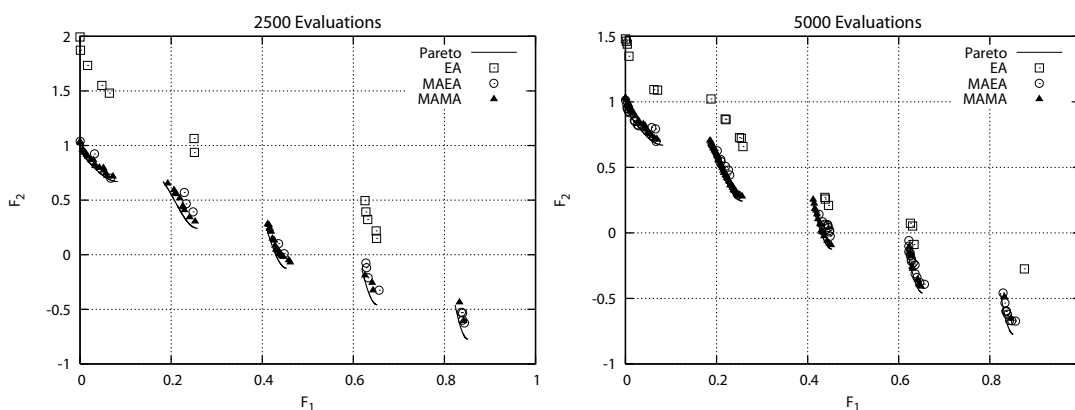


Figure 7. *ZDT3*: Fronts of the elite solutions for *EA*, *MAEA*, *MAMA* at the cost of 2500 (left) and 5000 (right) calls to the function evaluation tool for the best performing RNG seed. The exact Pareto front is also shown (continuous line).

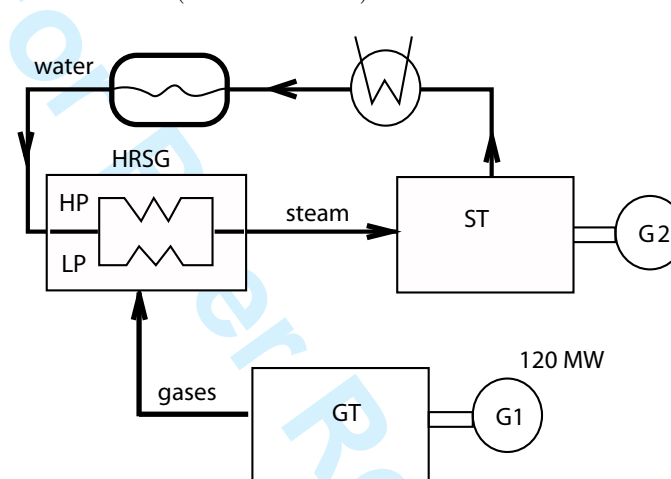


Figure 8. *Design of a CCPP*: Power plant configuration with a dual pressure heat recovery steam generator.

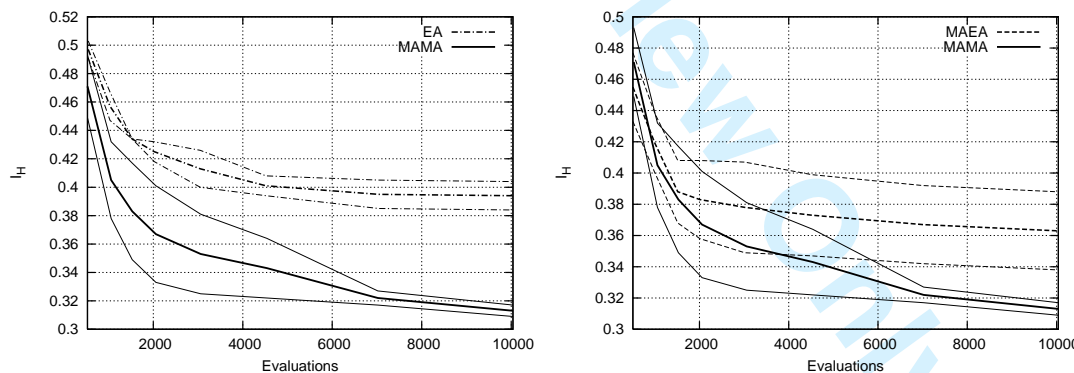


Figure 9. *Design of a CCPP*: Statistical measures for the performance of *EA* vs. *MAMA* (left) and *MAEA* vs. *MAMA* (right) for the three runs: average  $I_H$  values and the range of deviation (pairs of dashed lines) around the mean for a 66% probability are shown.

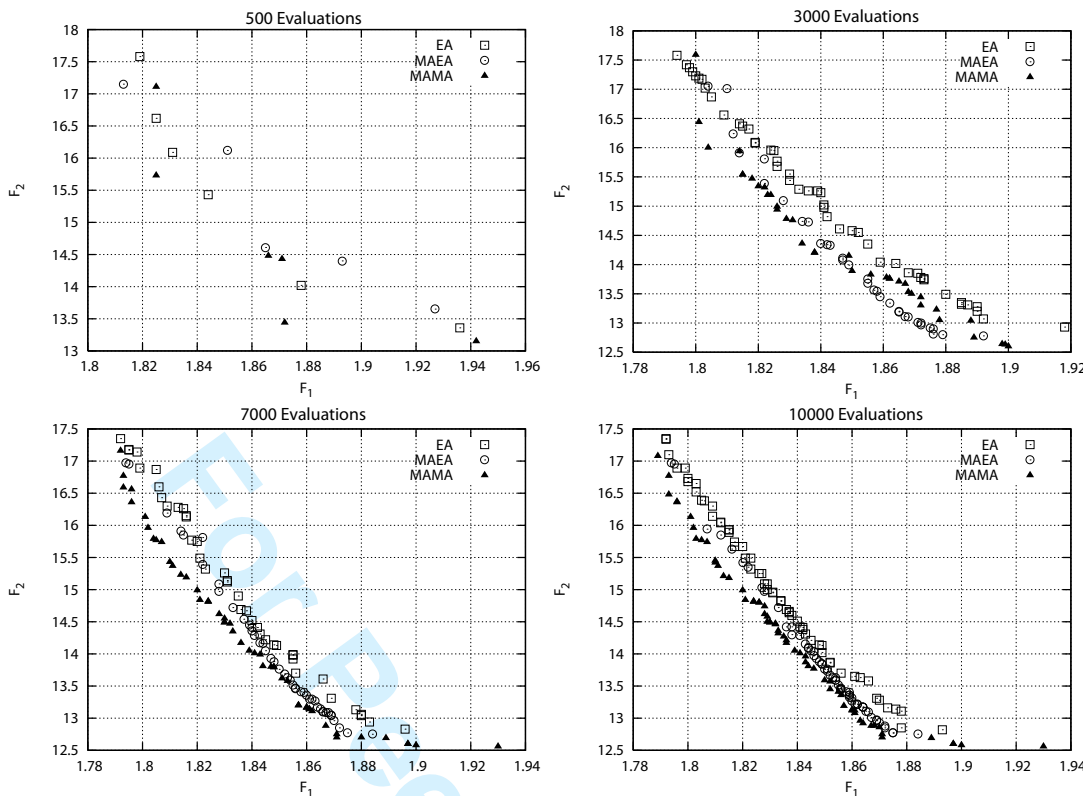


Figure 10. *Design of a CCPP*: Fronts of non-dominated solutions achieved using *EAs*, *MAEAs* and *MAMA* at 500, 3000, 7000 and 10000 exact evaluations.

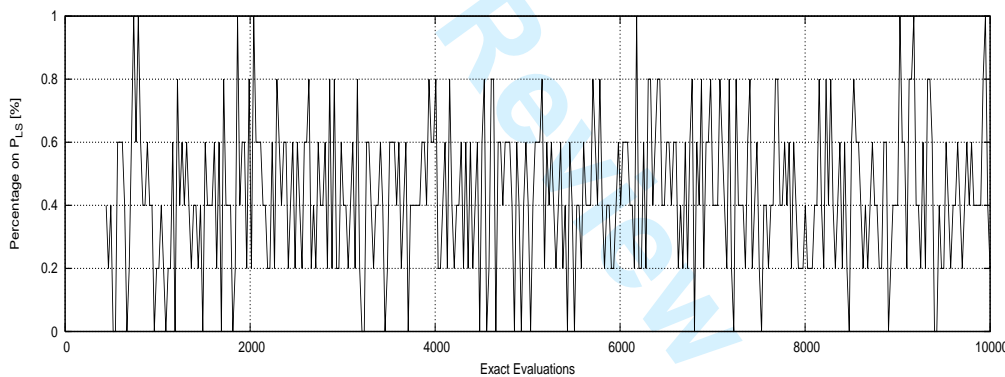


Figure 11. *Design of a CCPP*: *LS* statistics for the proposed *MAMA*: Percentage of totally or semi-improved (improved for all or at least one of the objectives, respectively) on the total number of individuals selected to undergo *LS*.

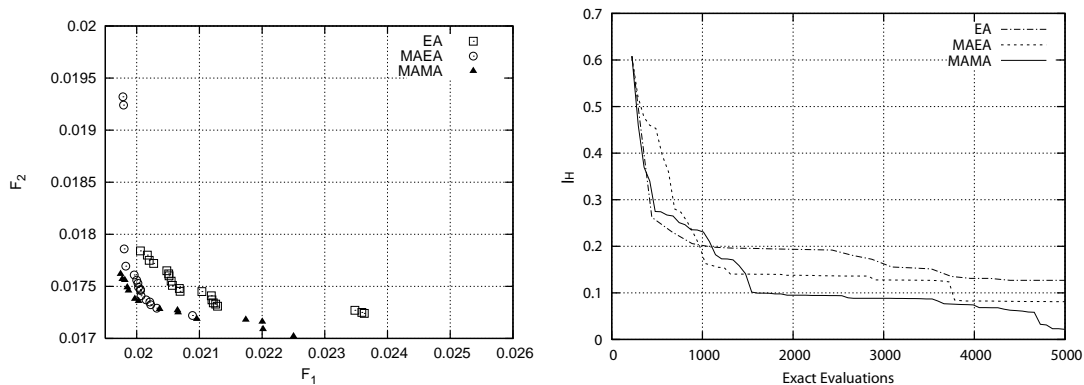


Figure 12. Design of a compressor cascade at two operating points: Left plot: Fronts of non-dominated solutions computed by the three methods at a cost of 5000 exact evaluations. Right plot: Convergence measured in terms of the dominated hypervolume  $I_H$ .

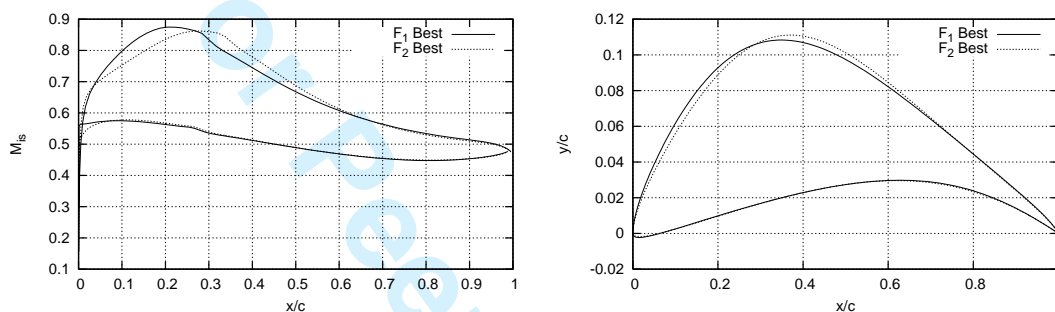


Figure 13. Design of a compressor cascade at two operating points: Comparison of the extreme Pareto individuals computed using MAMA at the cost of 5000 evaluations.

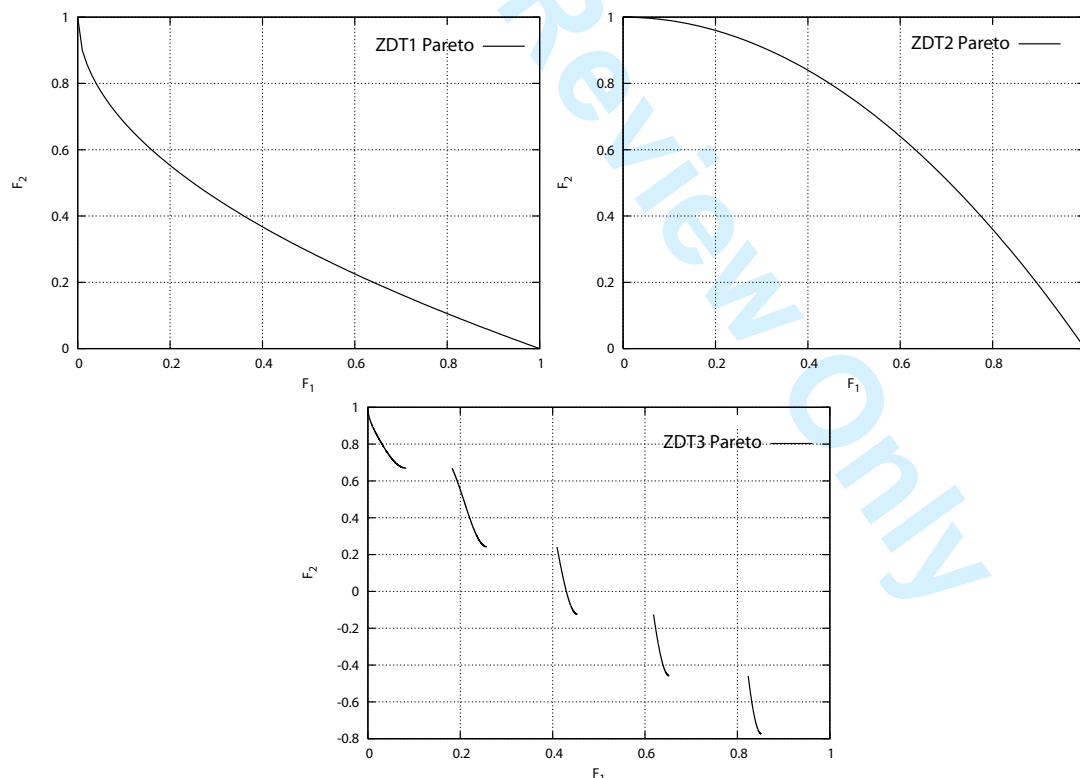


Figure 14. Mathematical Benchmarks: Analytical Pareto front of the ZDT1 (up-left), the ZDT2 (up-right) and the ZDT3 (low) test problems, gained by setting  $x_n = 0$ ,  $n = 2, N$ .

Table 1. *ZDT1*: Statistical measures for the performance of *EA*, *MAEA* and the proposed *MAMA* for the 25 runs: average, best, median and worst  $I_H$  values along with the standard deviation for 5000, 15000 and 25000 evaluations on the problem-specific tool are shown. Statistical t-tests prove that the proposed *MAMA* outperforms *EA* and *MAEA*, at any “instant” of the evolution.

Algorithm	Evaluations	Average	Stdev	Best	Median	Worst
<i>EA</i>	5000	0.144	0.009	0.128	0.150	0.165
	15000	0.088	0.003	0.083	0.088	0.093
	25000	0.080	0.002	0.077	0.080	0.083
<i>MAEA</i>	5000	0.094	0.004	0.088	0.096	0.102
	15000	0.076	0.001	0.074	0.077	0.079
	25000	0.073	0.001	0.071	0.073	0.075
<i>MAMA</i>	5000	0.071	0.001	0.070	0.072	0.074
	15000	0.069	0.0004	0.069	0.070	0.071
	25000	0.069	0.0004	0.069	0.069	0.070

Table 2. *ZDT2*: Statistical measures for the performance of *EA*, *MAEA* and the proposed *MAMA* for 25 runs: average, best, median and worst  $I_H$  values for 5000, 15000 and 25000 evaluations on the problem-specific tool are shown.

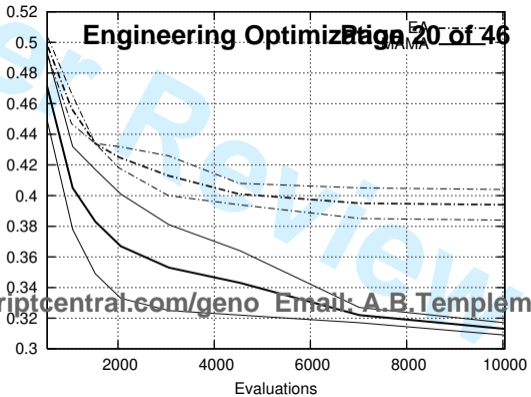
Algorithm	Evaluations	Average	Stdev	Best	Median	Worst
<i>EA</i>	5000	0.240	0.009	0.223	0.239	0.255
	15000	0.163	0.004	0.156	0.163	0.169
	25000	0.151	0.002	0.147	0.150	0.154
<i>MAEA</i>	5000	0.192	0.018	0.166	0.186	0.216
	15000	0.155	0.014	0.144	0.175	0.201
	25000	0.149	0.011	0.141	0.164	0.184
<i>MAMA</i>	5000	0.164	0.035	0.138	0.200	0.262
	15000	0.142	0.012	0.136	0.155	0.186
	25000	0.140	0.009	0.136	0.146	0.173

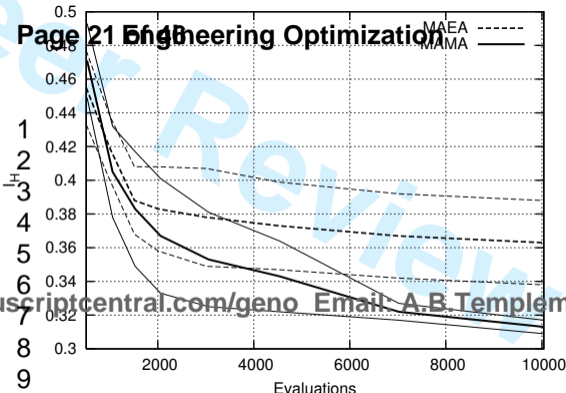
Table 3. *ZDT3*: Statistical measures for the performance of *EA*, *MAEA* and the proposed *MAMA* for 25 runs: average, best, median and worst  $I_H$  values for for 2500 and 5000 evaluations on the problem-specific tool are shown.

Algorithm	Evaluations	Average	Stdev	Best	Worst
<i>EA</i>	2500	0.27	0.04	0.23	0.31
	5000	0.19	0.02	0.17	0.21
<i>MAEA</i>	2500	0.16	0.03	0.13	0.22
	5000	0.14	0.02	0.12	0.22
<i>MAMA</i>	2500	0.13	0.02	0.12	0.16
	5000	0.12	0.01	0.11	0.13

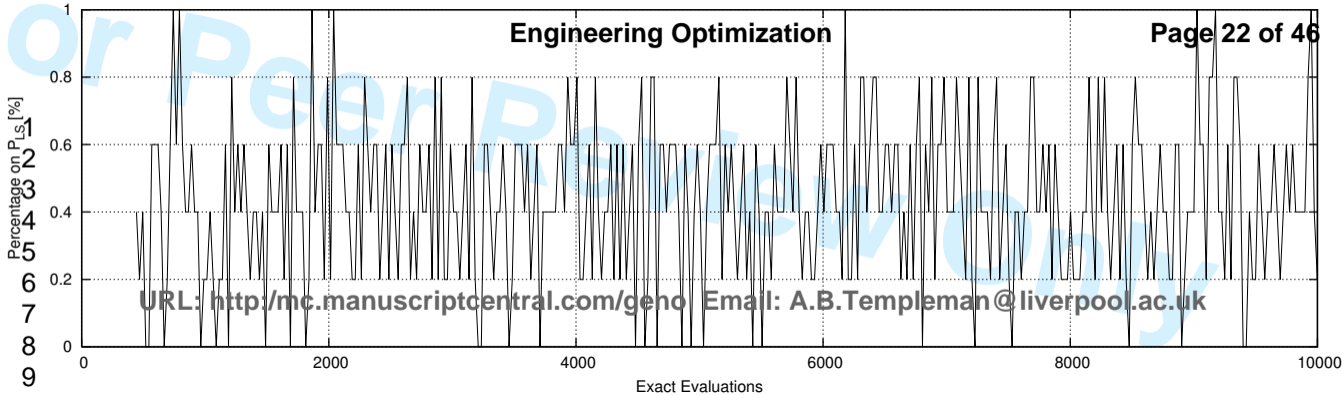
Table 4. *ZDT3*: Results of the t-test analysis (values of the  $t_0$  variable) for the three methods at several “instants” during the evolution, which prove that *MAMA* outperform *EA* and *MAEA* for a 99.9% probability.

	500	1500	2500	5000
MAMA vs. EA	9.2	12.4	13.0	8.5
MAMA vs. MAEA	5.5	4.2	4.1	4.5

1  
2  
3  
4  
5  
6  
7  
8  
9

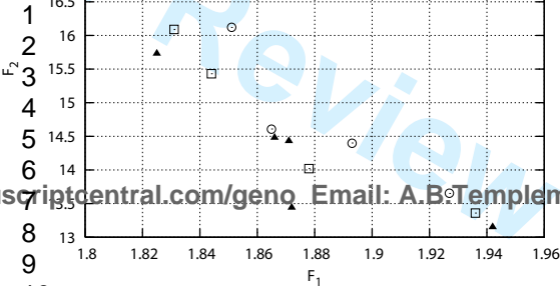


uscriptcentral.com/geno Email: A.B.Templem





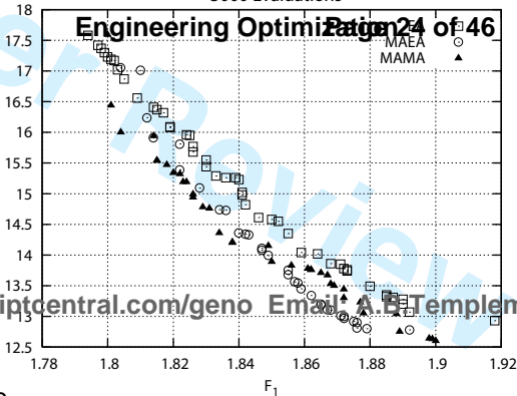
## Page 23 of 46 Engineering Optimization



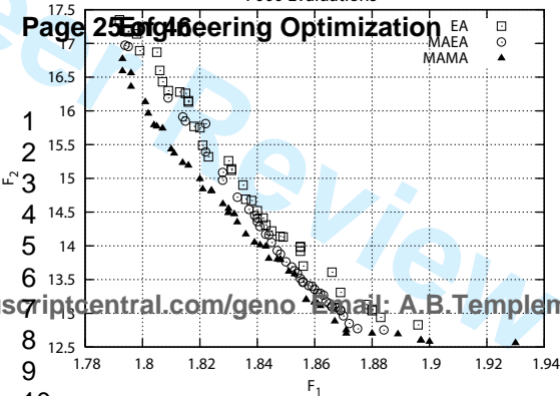
## Engineering Optimization 24 of 46

MAEA  
MAMA

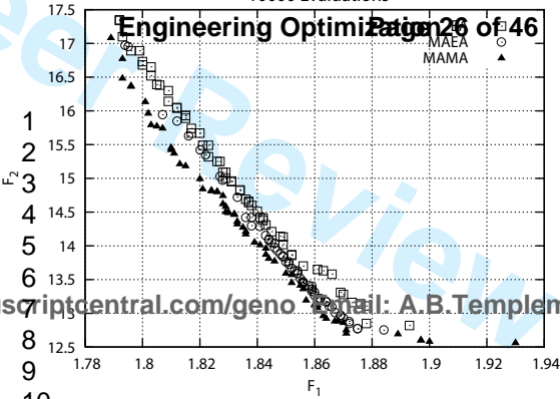
1  
2  
3  
4  
5  
6  
7  
8  
9  
10

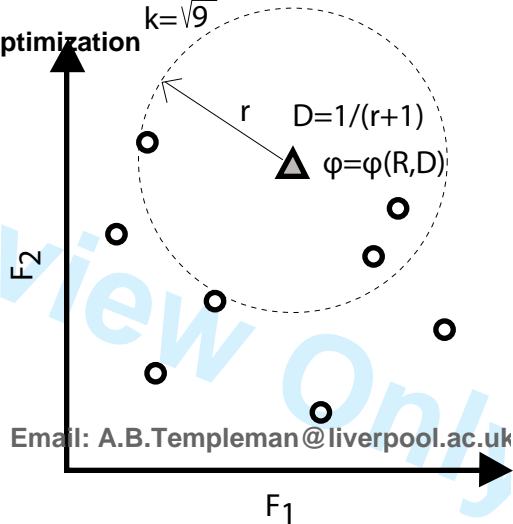
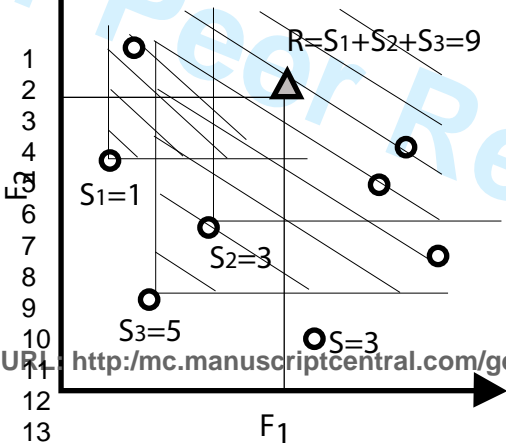


# Page 25 of 46 Bearing Optimization

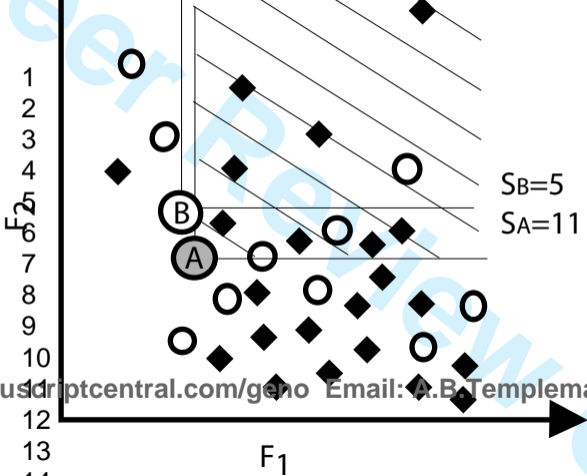


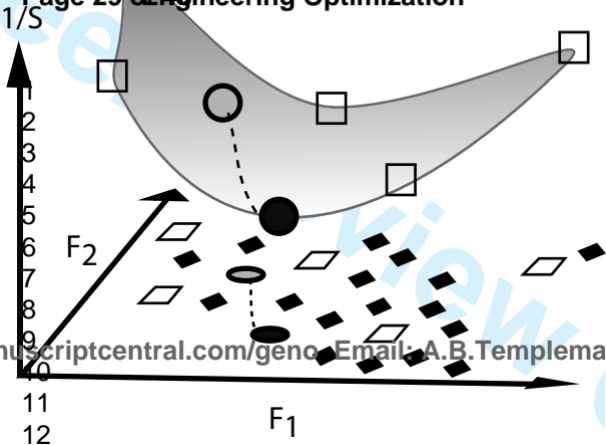
## Engineering Optimization 26 of 46

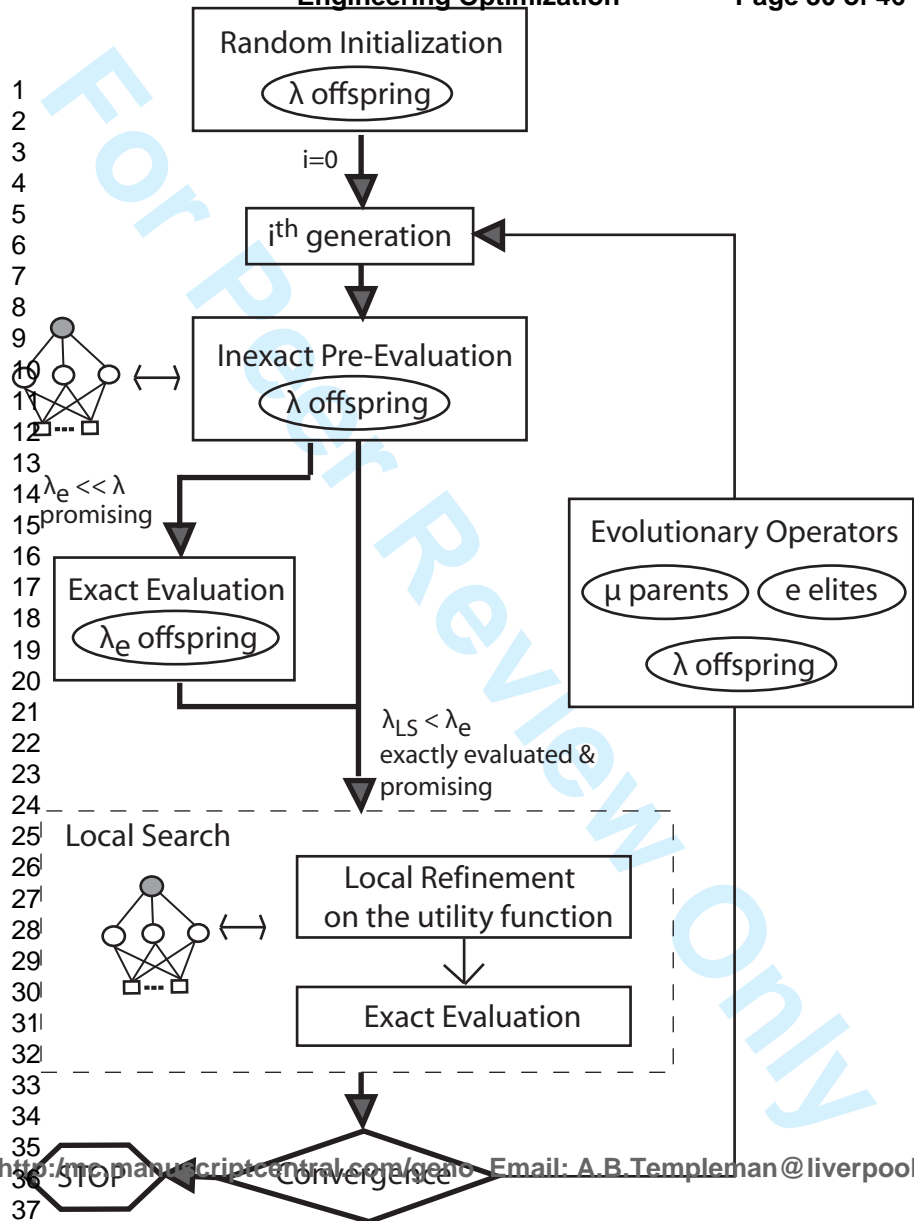




# Engineering Optimization Stage 28 of 46



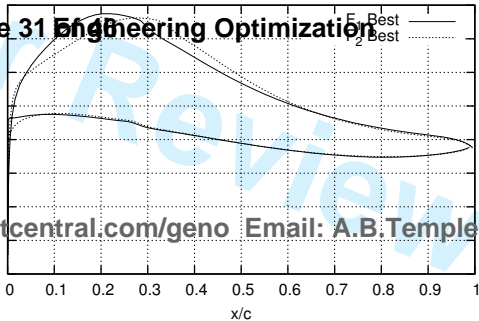






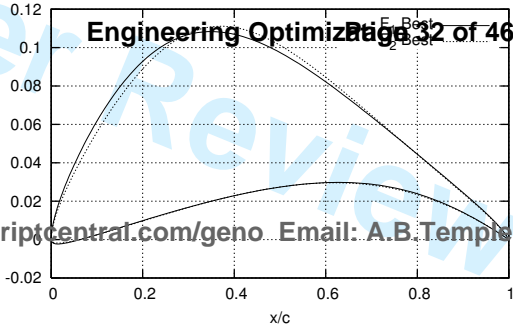
$F_1$  Best  
 $F_2$  Best

1  
2  
3  
4  
5  
6  
7



# Engineering Optimization Page 32 of 46

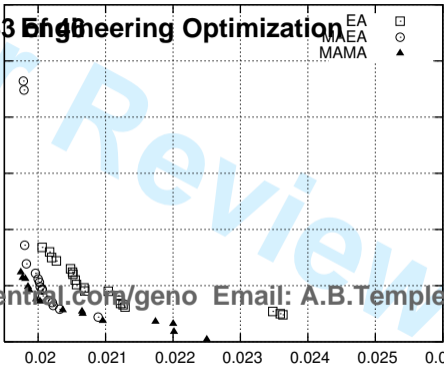
1  
2  
3  
4  
5  
6  
7

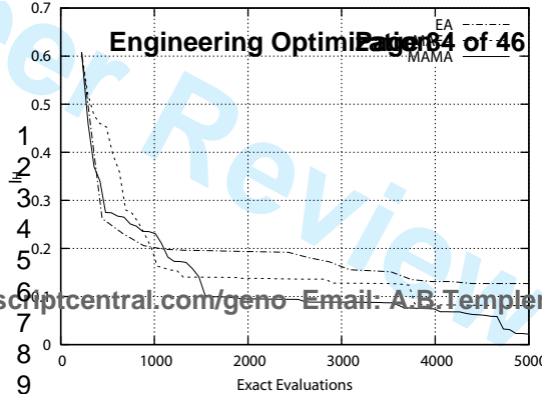


scriptcentral.com/geno Email: A.B.Templem

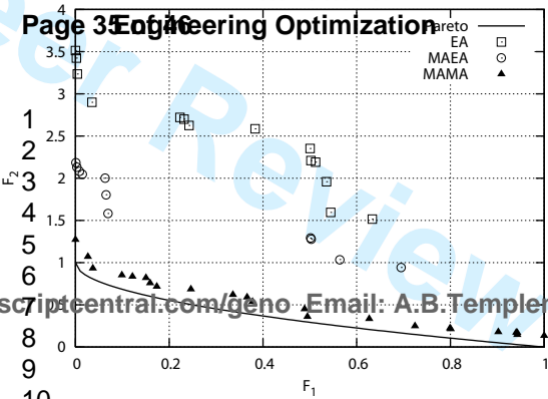
EA  $\square$   
MAEA  $\circ$   
MAMA  $\blacktriangle$

1  
2  
3  
4  
5  
6  
7  
8  
9



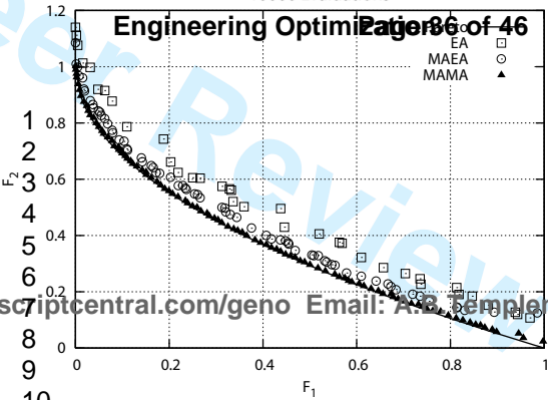


# Page 35 Engineering Optimization

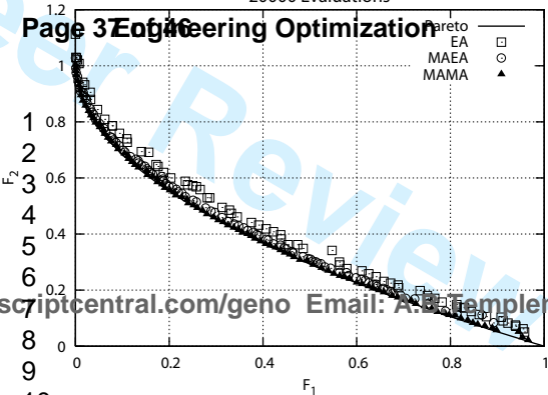


## Engineering Optimizer 86 of 46

EA  $\square$   
MAEA  $\circ$   
MAMA  $\blacktriangle$



## Page 3 of 16 Engineering Optimization

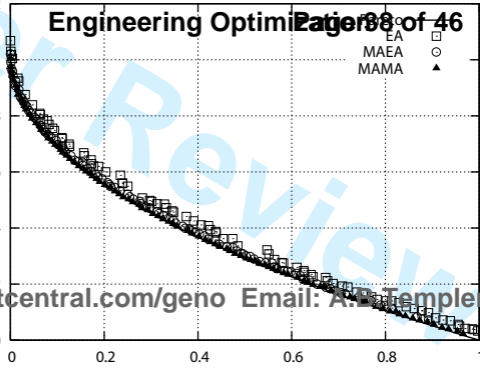


25000 Evaluations

# Engineering Optimization 38 of 46

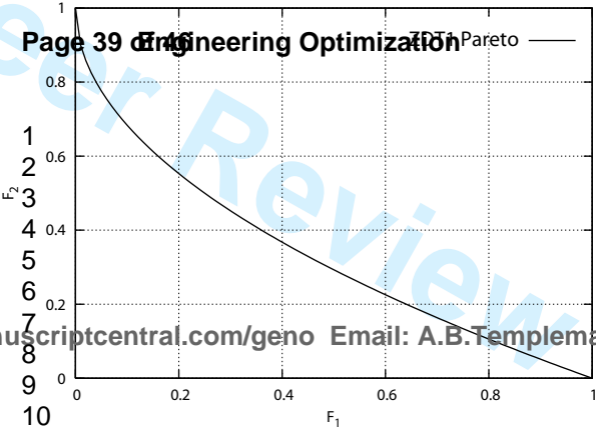
1  
2  
3  
4  
5  
6  
7  
8  
9  
10

EA  $\square$   
MAEA  $\circ$   
MAMA  $\blacktriangle$



scriptcentral.com/geno Email: A.B.Templer

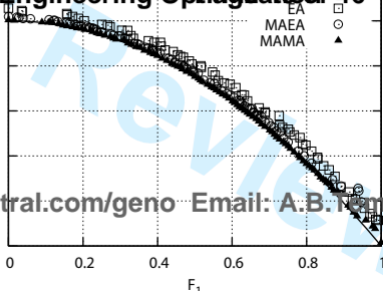




25000 Evaluations

# Engineering Optimization of 46

F<sub>2</sub>  
1  
2  
3  
4  
5  
6  
7

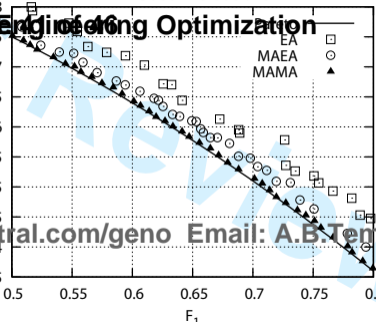


central.com/geno Email: A.B.Tem

25000 Evaluations

# PageRanking Optimization

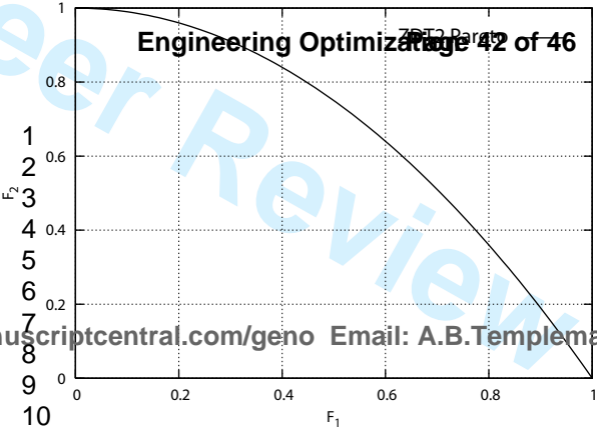
1  
2  
3  
4  
5  
6  
7



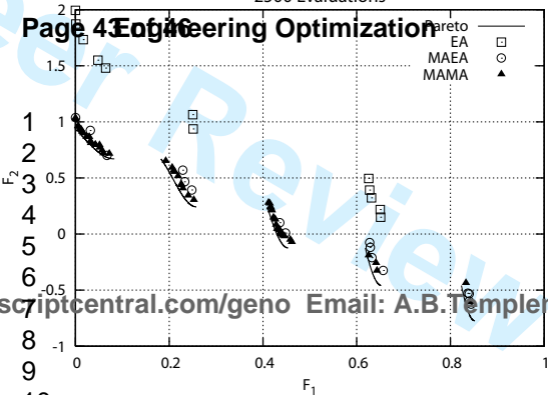
ptcentral.com/geno Email: A.B.Tem

# Engineering Optimization Page 42 of 46

ZDT2 Parato



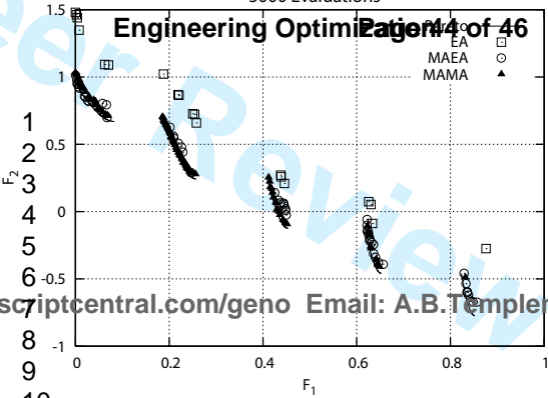
## Page 43 Engineering Optimization

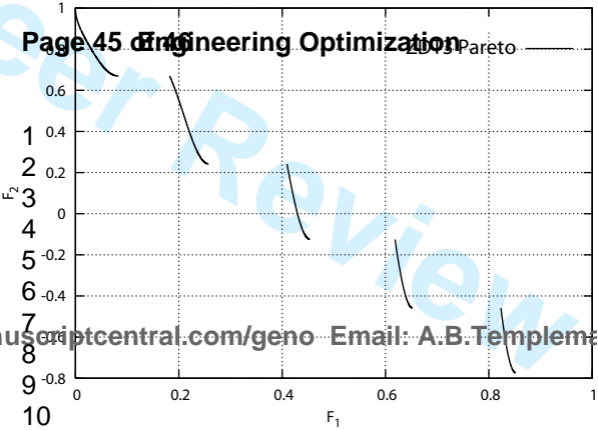


5000 Evaluations

# Engineering Optimization

Page 4 of 46





water

Engineering Optimization

Page 46 of 46

